AGU PUBLICATIONS

Geophysical Research Letters

RESEARCH LETTER
10.1002/2016GL068378

Key Points:
- Earthflow velocities reached a historic low in the extreme 2012–2015 drought
- Earthflow deceleration initiated around 2000 with the onset of drought
- The sensitivity of earthflow velocity to climate depends on earthflow thickness

Supporting Information:
- Supporting Information S1

Correspondence to:
G. L. Bennett,
georgieb@colostate.edu

Citation:
Bennett, G. L., J. J. Roering, B. H. Mackey, A. L. Handwerger, D. A. Schmidt, and B. P. Guillod (2016), Historic drought puts the brakes on earthflows in Northern California, *Geophys. Res. Lett.*, *43*, 5725–5731, doi:10.1002/2016GL068378.

Received 24 FEB 2016
Accepted 2 MAY 2016
Published online 1 JUN 2016

Historic drought puts the brakes on earthflows in Northern California

G. L. Bennett[1,2], J. J. Roering[1], B. H. Mackey[1], A. L. Handwerger[1], D. A. Schmidt[3], and B. P. Guillod[4]

[1]Department of Geological Sciences, University of Oregon, Eugene, Oregon, USA, [2]Now at Department of Geosciences, Colorado State University, Fort Collins, Colorado, USA, [3]Department of Earth and Space Sciences, University of Washington, Seattle, Washington, USA, [4]Environmental Change Institute, University of Oxford, Oxford, UK

Abstract California's ongoing, unprecedented drought is having profound impacts on the state's resources. Here we assess its impact on 98 deep-seated, slow-moving landslides in Northern California. We used aerial photograph analysis, satellite interferometry, and satellite pixel tracking to measure earthflow velocities spanning 1944–2015 and compared these trends with the Palmer Drought Severity Index, a proxy for soil moisture and pore pressure that governs landslide motion. We find that earthflow velocities reached a historical low in the 2012–2015 drought, but that their deceleration began at the turn of the century in response to a longer-term moisture deficit. Our analysis implies depth-dependent sensitivity of earthflows to climate forcing, with thicker earthflows reflecting longer-term climate trends and thinner earthflows exhibiting less systematic velocity variations. These findings have implications for mechanical-hydrologic interactions that link landslide movement with climate change as well as sediment delivery in the region.

1. Introduction

Drought is an increasing global phenomenon [*Dai*, 2013] driven by precipitation deficits over periods of years and amplified by increasing temperatures. California's early 21st century drought reached historic proportions in 2015 with 2012–2015 constituting a drought that is unprecedented in the state's historical record [*Robeson*, 2015]. Widespread consequences of the drought on the state's resources and population include a reduction in water supply and crop yields [*Cooley et al.*, 2015], groundwater depletion [*Borsa et al.*, 2014], widespread forest mortality [*Asner et al.*, 2016], and increased wildfire risk. A special issue in *Geophysical Research Letters* delves deeper into the drought, its origins, and consequences [*Swain*, 2015], but little has been reported on geomorphic response to drought, either in California or elsewhere [e.g., *McSaveney and Griffiths*, 1987]. Here we utilize a novel combination of historic photoanalysis, automated satellite pixel tracking, and satellite interferometry (interferometric synthetic aperture radar (InSAR)) to assess the response of multiple landslides to drought in Northern California.

Understanding and predicting landslide response to climate change are a significant challenge for Earth scientists with implications for infrastructure and population centers globally. Although individual landslide events tend to have relatively small impacts compared to other hazards such as earthquakes and floods, landslides kill at least 5000 people a year globally [*Petley*, 2012] and cost an estimated $20 billion dollars or 17% of the annual losses from all natural disasters [*Klose*, 2015]. Much research on landslide response to climate surrounds their response to extreme rainfall events [e.g., *Guzzetti et al.*, 2007] and melting permafrost [e.g., *Gruber*, 2004], both of which are predicted to increase with climate change. However, landslide response to drought, which is also predicted to increase [*Dai*, 2013], remains largely unexplored; *McSaveney and Griffiths* [1987] provide one of the few assessments of landslide response to drought. Further research on landslide response to drought as a climatic forcing event is needed to better understand the variable response of landslides, and more generally, geomorphic and hydrologic processes to climate change [*Pelletier et al.*, 2015].

Deep-seated (>5 m), slow-moving (<4 m yr^{-1}) landslides, often referred to as earthflows [*Hungr et al.*, 2014], respond to changes in precipitation [*Baum and Reid*, 2000; *Iverson and Major*, 1987] through pore water pressures at the basal shear surface [*Schulz et al.*, 2009; *Terzaghi*, 1950; *Van Asch et al.*, 1999], which are controlled by groundwater dynamics [*Iverson and Major*, 1987]. Over time scales of >1 year, earthflow movement has been shown to be well correlated with surface moisture balance as expressed by indices such as the Moisture Balance Drought Index, suggesting these to be useful proxies for basal pore pressures [*Coe*, 2012].

This hydrologic linkage is supported by data of *Iverson and Major* [1987] showing the correspondence of near-surface (~2 m) and deep (~10 m) groundwater levels, determined from wells in Minor Creek landslide in Northern California. Numerical models and field-based measurements suggest that increases in pore water pressure that drive landslide motion predominantly diffuse vertically through the earthflow body from the surface and can be approximated by a 1-D linear diffusion model [*Berti and Simoni*, 2010, 2012; *Iverson and Major*, 1987]. On this basis, landslides should respond to changing soil moisture as a function of their thickness, although values of the relevant hydrologic parameters remain unclear [*Handwerger et al.*, 2013].

Here we compare the movement of multiple earthflows in Northern California over seven decades (1944–2015) with the Palmer Drought Severity Index (PDSI), a surface moisture balance index and the most prominent index of meteorological drought in the U.S. We further explore earthflow response to the 2012–2015 drought as a function of earthflow thickness, which may reflect hydrologic-mechanical linkages.

2. Study Site

We focus on a 140 km^2 area of the Eel River catchment containing 98 active earthflows originally mapped by *Mackey and Roering* [2011]. The site is located within the Central Belt of the Franciscan mélange, a highly sheared, Jurassic-Cretaceous accretionary prism complex within the Northern Californian Coast Range. As is typical of mountainous regions with weak mélange lithology, erosion and landscape evolution in the region is dominated by earthflows. Although slow-moving (0.2–4.2 m yr^{-1}), these features contribute >50% of the total erosion in the region [*Bennett et al.*, 2016; *Kelsey*, 1978; *Mackey and Roering*, 2011]. Comprehensive landslide mapping has revealed this stretch of the Eel River to have the highest earthflow erosion rates in the region due to rapid rock uplift (~1 mm yr^{-1}) related to the migration of the Mendocino Triple Junction [*Bennett et al.*, 2016].

Precipitation is highly seasonal with most of the 1.4 m of annual precipitation falling between October and April. Surprisingly, earthflows in the region appear to respond to seasonal precipitation in a remarkably synchronous fashion (within approximately 40 days following the onset of rainfall) despite a nearly order of magnitude variation in thickness [*Handwerger et al.*, 2013]. A detailed study of one earthflow in the region shows its slow-down over the late 20th century, interpreted as a possible response to climate change or decline in supply of landslide material from the headscarp region [*Mackey et al.*, 2009]. Meteoric ^{10}B analysis of the same earthflow shows that it has experienced movement for at least 150 years, indicating that earthflows can sustain perpetual movement for long periods of time [*Mackey et al.*, 2009].

3. Methods

We combined manual mapping and automated pixel tracking to obtain earthflow velocities across our study site spanning 1944–2015. First, we calculated mean 1944–2006 earthflow velocities for 98 earthflows by averaging tree displacements mapped from aerial photographs by *Mackey and Roering* [2011] for each earthflow. *Mackey et al.* [2009] conducted more detailed mapping of tree displacements for one of these earthflows (referred to as "Kekawaka" by *Mackey et al.* [2009] and "Kekawaka 2" by *Handwerger et al.* [2013, 2015] and in this study) from more closely spaced aerial photographs between 1944 and 2006. We selected an additional nine earthflows to conduct more detailed mapping from a sequence of orthorectified aerial photographs [*Mackey et al.*, 2009; *Mackey*, 2009; Table S1]. Combining our nine earthflow velocity time series with that of *Mackey et al.* [2009] yields 10 earthflow time series for 1944–2006 with an average temporal resolution of 9 years with which to investigate decadal velocity patterns.

Second, we measured the velocities of all 98 earthflows for the periods 2009–2012 and 2012–2015 using automated pixel tracking. Notably, the latter period coincides with the period of unprecedented drought [*Robeson*, 2015]. We conducted our analysis in the COSI CORR software package [*Leprince et al.*, 2007] from 0.5 m resolution Worldview satellite imagery. COSI CORR can measure millimeter-scale surface deformation from optical imagery and has been widely and successfully applied to the study of fault displacement [e.g., *Hollingsworth et al.*, 2012], regional glacier velocities [e.g., *Scherler et al.*, 2011], and individual landslides [*Leprince et al.*, 2008; *Roering et al.*, 2015; *Stumpf et al.*, 2014]. We chose Worldview satellite imagery for its spatial and temporal coverage of the study site and high resolution (0.5 m), obtaining three panchromatic

images for 2009, 2012, and 2015 and a stereo pair for 2014 (Table S2 in the supporting information). Multitemporal images acquired at different viewing angles require both orthorectification with an accurate digital elevation model (DEM) and coregistration, prior to their correlation in COSI CORR. We followed the same procedure for image orthorectification and coregistration as *Stumpf et al.* [2014], performing our processing in the ERDAS Imagine software package.

We correlated our orthorectified, co-registered images with COSI CORR to obtain displacements for the periods 2009–2012 and 2012–2015. COSI CORR measures displacements in the north-south and east-west directions, which are combined to produce displacement fields. Our error analysis followed three steps, estimation, and removal of systematic error in the displacement fields (Figures S1 and S2 in the supporting information), filtering to reduce noise, and validation of our measured displacements based on coincident InSAR measured displacements for a subset of earthflows [*Handwerger et al.*, 2015] (Figure S3). On the basis of poor 2015 image quality and noise in the resulting displacement 2012–2015 field, we also produced a displacement field for 2012–2014.

While earthflows are known to have different kinematic zones [e.g., *Handwerger et al.*, 2015], we are interested in the bulk earthflow behavior and thus calculated mean earthflow velocity as the mean displacement ($\geq$0) within the entire earthflow body as mapped by *Mackey and Roering* [2011]. We estimated that the remaining random error in our displacement fields (Figure S2) contributes to an uncertainty on the order of $\pm 0.02\,\mathrm{m\,yr^{-1}}$ when averaged over an earthflow. This is consistent with error in the manual measurements [*Mackey et al.*, 2009]. Finally, we omitted 5 of the 98 earthflows, including 2 of our 10 focus earthflows, from further analysis for 2012–2015 on the basis of high nonsystematic error in the displacement field (Figure S1c).

In order to assess the response of earthflows to the 2012–2015 drought, we compared the velocity time series of our 10 focus earthflows with annual mean Palmer Drought Severity Index (PDSI) downloaded from the National Climate Data Center of NOAA for division 1 in California (Figure S4). PDSI is the most prominent index of meteorological drought used in the United States [*Palmer*, 1965] and was used to demonstrate the extreme and unprecedented nature of the 2012–2015 drought in California [*Robeson*, 2015]. It incorporates antecedent moisture conditions, precipitation, and potential evapotranspiration into a surface moisture balance. It is a standardized measure, ranging from -10 (dry) to +10 (wet), with values < -3 representing severe to extreme drought. *Dai et al.* [2004] and *Dai* [2011] showed that PDSI is significantly correlated with measured soil moisture as well as satellite observations of water storage over many parts of the world, including the U.S. We tested its suitability for representing surface (~2 m) soil moisture at our study site by comparing PDSI with soil moisture estimates from phase 2 of the North American Land Data Assimilation System (NLDAS-2) [*Xia et al.*, 2012]. A strong positive relationship ($R^2 = 0.7$; Figure S5) suggests that PDSI adequately represents soil moisture at our study site and is a useful proxy of pore pressure relevant for earthflow movement.

Finally, we investigated the relationship between earthflow velocity and PDSI as a function of earthflow thickness. We use the terms thickness and depth interchangeably throughout the text to refer to the average depth from earthflow surface to the basal shear zone. Mean earthflow basal depths of 69 of our earthflows were approximated from field and lidar calculations of earthflow toe height at the channel interface and depth of gully incision through the earthflow body [*Handwerger et al.*, 2013; *Mackey and Roering*, 2011]. These depths are minimum estimates as gullies and channels are not typically fully incised through the landslide mass. Thicknesses of our remaining 29 earthflows were approximated from earthflow areas using an empirical scaling relationship developed for earthflows in the study area [*Handwerger et al.*, 2013], $D = \alpha A^{\gamma}$, where D is earthflow depth, A is earthflow planform area, $\alpha = 0.46$, $\gamma = 0.29$, and the r^2 value of the relationship is 0.45.

4. Results

The mean velocity of all 98 earthflows decreased by more than 50% from 0.27 (0.02) $\mathrm{m\,yr^{-1}}$ in 1944–2006 to 0.12 (0.02) $\mathrm{m\,yr^{-1}}$ in 2009–2012 and subsequently more than halved again to 0.04 (0.01) $\mathrm{m\,yr^{-1}}$ in 2012–2015 (Figure 1), where value in parentheses reports standard error. Considering only earthflows above our estimated error of $0.02\,\mathrm{m\,yr^{-1}}$, ~25% of earthflows active in 1944–2006 exhibited

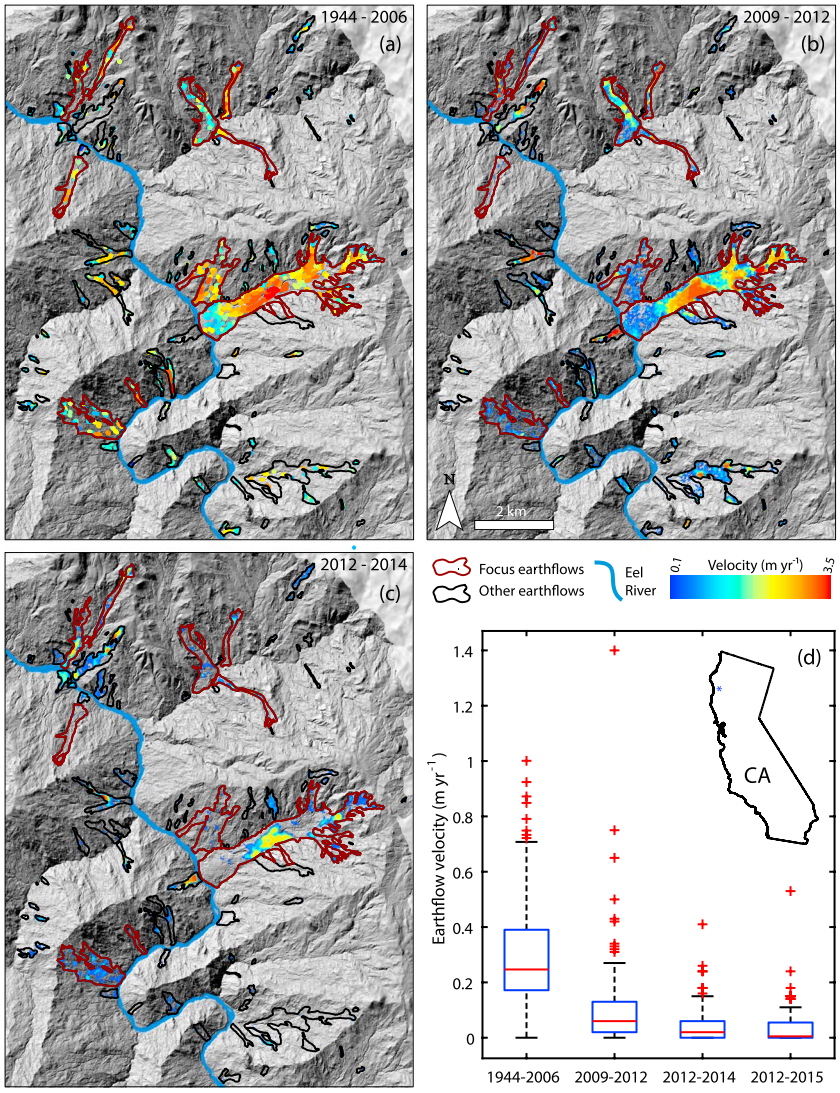

Figure 1. Earthflow displacement fields clipped by earthflow polygons measured for the 98 earthflows found by (a) manually tracking of trees on sequential aerial photographs for the period 1944–2006 [*Mackey and Roering*, 2011], (b) automatically using pixel tracking for 2009–2012, and (c) 2012–2014. Focus earthflows are a subset of 10 of the 98 earthflows with velocities measured at a higher temporal resolution over the 1944–2006 period (Figure 2a). (d) Mean earthflow velocities, including those measured from the 2012–2015 displacement map (Figure S1c), along with an inset location map of the study site (blue star) in California. The central horizontal red line in box plot is the median, the edges of the blue box are the 25th and 75th percentiles, the whiskers extend to 1.5 times the interquartile range, and the red crosses depict outliers.

undetectable motion between 2009 and 2012. A further 40 earthflows or ~50% of those still active in 2009–2012 exhibited undetectable motion ($\leq$0.02 m yr^{-1}) in 2012–2014 (Figure S6). While the recent decrease in earthflow velocities has been particularly rapid, it is part of a long-term slowing trend commencing in the mid-late 1990s (Figure 2a).

The mean earthflow velocity of our 10 focus earthflows was relatively steady until the late 1990s when deceleration ensued (Figure 2a), coincident with the onset of drought conditions (PDSI $<$ 0) (Figure 2b). Although the recent 15 year period dominated by negative multiyear averaged PDSI values included a few years with slightly positive PDSI values in 2005 and 2010, the average velocity of our studied earthflows has continually decelerated since the turn of the century, reaching a historic low in the extreme 2012–2015 drought [*Robeson*, 2015]. Although the sparse nature of our data precludes a rigorous correlation, the general correspondence of our velocity data with 9 year average PDSI values implies that earthflows may respond to climate trends beyond

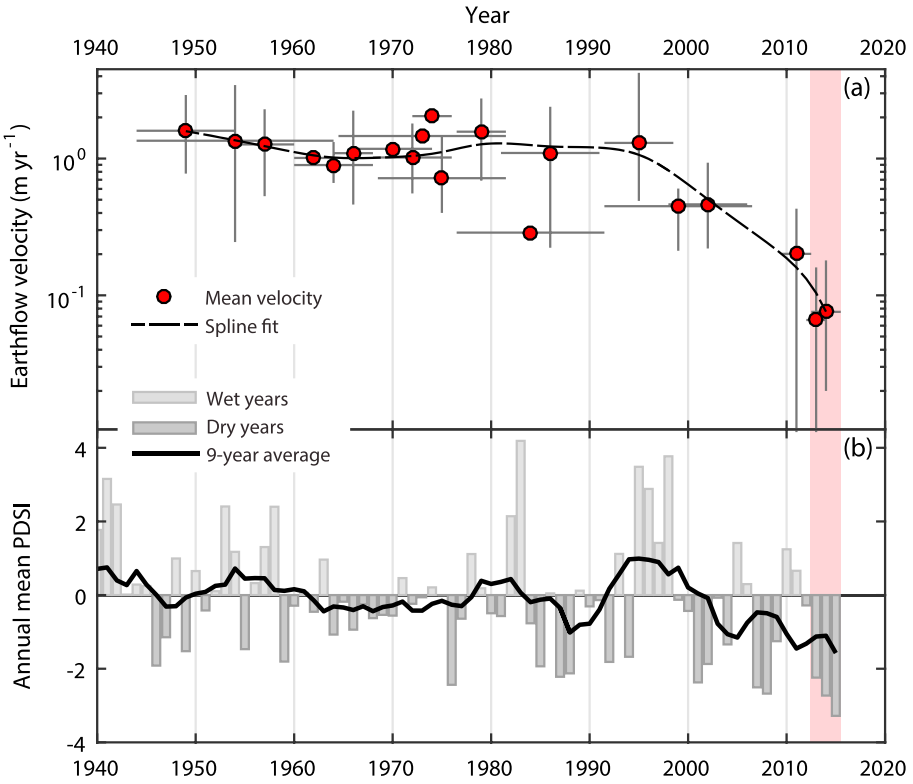

Figure 2. (a) Earthflow velocities for our 10 focus earthflows. The vertical bars around the means represent the range of velocities for each earthflow measured for the time intervals represented by the horizontal bars. Not all earthflows were identifiable in every set of aerial photographs, leading to several overlapping measurement intervals. The number of earthflows for each period (n) varies due to variable photo coverage of earthflows. Spline fit only considers mean earthflow velocities where $n > 1$ for a given measurement interval. (b) Annual mean PDSI fit with a 9 year centered moving average (black line). The pink bar highlights the most recent drought cycle.

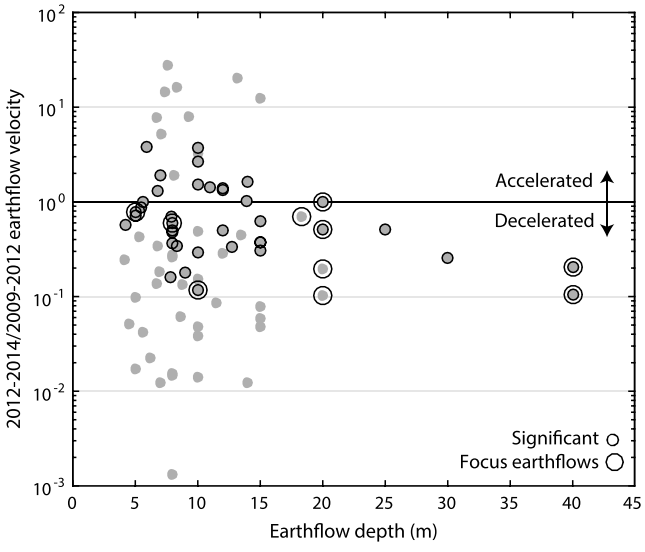

Figure 3. Landslide velocity changes between 2009–2012 and 2012–2014 as a function of earthflow depth; see also Figure S6. Significant earthflows had mean velocities >0.02 m yr^{-1} in both periods (greater than velocities that may arise from random error alone) in both periods. Error in individual earthflow depths is estimated to be 25% [*Mackey and Roering*, 2011].

the time scale of storms or even seasonal rainfall. Alternative factors that may influence earthflow motion, such as grazing, road construction, forestry, and fire, do not exhibit systematic temporal variations in our study area.

We further explored earthflow sensitivity to climate forcing as a function of earthflow depth, focusing on velocity changes that occurred during the recent extreme drought. Figure 3 shows that the 89 earthflows <15 m thick showed high-velocity variability between 2009–2012 and 2012–2014. Twenty-four (13) accelerated and 74 (25) decelerated by up to 3 (1) orders of magnitude, with values in brackets referring to earthflows displaying significant changes. In contrast,

the nine thicker earthflows (>15 m) uniformly decelerated and showed less variability in their deceleration, slowing by a maximum of 1 order of magnitude.

5. Discussion and Conclusions

Results from this study are the first to document the geomorphic response to historic drought in California. While deceleration of earthflows in response to the recent (2012–2015) drought has been particularly rapid, we find that the vast majority of earthflows along the Eel River catchment have been decelerating since the turn of the century coinciding with a longer-term moisture deficit in the region. We also observe the depth-dependent sensitivity of landslides to climate forcing for the first time. Our findings have implications for understanding mechanical-hydrologic controls on earthflow movement in the Eel River and beyond as well as for understanding and predicting the variable response of landslides to climate change.

Earthflows <15 m deep both accelerated and decelerated in the 2012–2015 drought, such that they do not consistently slow down with the extreme drought conditions, as thicker earthflows appear to do. One potential explanation is that individual storms may influence shallow landslides within this period owing to shallow (and relatively rapid) perturbations to the groundwater regime [e.g., *Iverson and Major*, 1987]. Alternatively, shallow landslide movement may be influenced by groundwater conditions that are relatively independent of long-term climate and thus hydrologic trends, for example, through development of perched water tables. Furthermore, the variable response of these shallow features may have been affected by changes in vegetation, resupply of material to the landslide by failures at the headscarp, or other changes in landslide structure and hydrologic parameters [*Mackey et al.*, 2009].

The consistent deceleration of thicker (>15 m) earthflows in the 2012–2015 drought suggests that these earthflows may be relatively insensitive to annual and subannual fluctuations and instead track changes in longer-term moisture balance at time scales of >2 years. This inference is consistent with the broad correspondence of the mean velocity of our 10 focus earthflows, 7 of which are >15 m thick, with decadal average PDSI. Our results have implications for predicting landslide movement based on climate predictions [e.g., *Coe*, 2012]. While deeper earthflows may reflect long-term climate trends, our results suggest that accurate prediction of shallow landslide response will be complicated as evidenced by their high variability.

The depth-dependent response of earthflows to multiannual climate forcing presented here differs from the depth-independent response of earthflows to the onset of seasonal rainfall [*Handwerger et al.*, 2013]. However, these differences in landslide behavior are not necessarily contradictory. As noted by *Handwerger et al.* [2013], it is possible that earthflow response time to onset of seasonal rainfall is less than the ~40 day resolution of their InSAR data, precluding observation of variability in earthflow response time as a function of earthflow depth. Alternatively, it is possible that seasonal earthflow response is superimposed on longer-term decadal earthflow response to climate forcing.

It will be both illuminating and important to continue to monitor these earthflows as rainfall returns, particularly given the hypothesis that extreme drying may increase pathways for runoff into earthflows through development of cracks [*Krzeminska et al.*, 2013; *McSaveney and Griffiths*, 1987]. Catastrophic failure of earthflows is not common but the current extreme drought may generate an unprecedented, nonlinear response [*Pelletier et al.*, 2015].

Acknowledgments
We are grateful to two anonymous reviewers for comments that helped to improve the paper, as well as to Editor M. Bayani Cardenas. Thanks to André Stumpf for advice on image coregistration and DEM extraction and to Sebastien LePrince, Corina Cerovski-Darriau, and William Armstrong for COSI-CORR discussions and advice. Worldview imagery was provided by the National Geospatial Intelligence Agency (NGA). Thanks especially to Jaime Nickeson at NASA. Research largely funded by NASA grants NNX12AL93G and NNX08AF95G.

References

Asner, G. P., P. G. Brodrick, C. B. Anderson, N. Vaughn, D. E. Knapp, and R. E. Martin (2016), Progressive forest canopy water loss during the 2012–2015 California drought, *Proc. Natl. Acad. Sci. U.S.A.*, *113*(2), E249–E255, doi:10.1073/pnas.1523397113.

Baum, R. L., and M. E. Reid (2000), Ground water isolation by low-permeability clays in landslide shear zones, in *Landslides in Research, Theory and Practice, Proceedings of the 8th International Symposium on Landslides Cardiff, Wales*, vol. 1, edited by E. Bromhead, N. Dixon, and M. Ibsen, pp. 139–144, Thomas Telford, London.

Bennett, G. L., S. R. Miller, J. J. Roering, and D. A. Schmidt (2016), Landslides, threshold slopes and the survival of relict terrain in the wake of the Mendocino Triple Junction, *Geology*, *44*, 363–366, doi:10.1130/G37530.1.

Berti, M., and Simoni, A. (2010), Experimental evidence of pore pressure diffusion in clayey soils prone to landsliding, *J. Geophys. Res.*, *115*, F03031, doi:10.1029/2009JF001463

Berti, M., and A. Simoni (2012), Observation and analysis of near-surface pore-pressure measurements in clay-shales slopes, *Hydrol. Processes*, *26*(14), 2187–2205, doi:10.1002/hyp.7981.

Borsa, A. A., D. C. Agnew, and D. R. Cayan (2014), Ongoing drought-induced uplift in the western United States, *Science*, *345*(6204), 1587–1590, doi:10.1126/science.1260279.

Coe, J. A. (2012), Regional moisture balance control of landslide motion: Implications for landslide forecasting in a changing climate, *Geology*, *40*(4), 323–326, doi:10.1130/G32897.1.
Cooley, H., K. Donnelly, R. Phurisamban, and M. Subramanian (2015), Impacts of California's Ongoing Drought: Agriculture, (August) 30. [Available at http://pacinst.org/publication/impacts-of-californias-ongoing-drought-agriculture/.]
Dai, A. (2011), Characteristics and trends in various forms of the Palmer Drought Severity Index during 1900–2008, *J. Geophys. Res.*, *116*, D12115, doi:10.1029/2010JD015541
Dai, A. G. (2013), Increasing drought under global warming in observations and models, *Nat. Clim. Change*, *3*(1), 52–58, doi:10.1038/nclimate1633.
Dai, A., K. E. Trenberth, and T. Qian (2004), A global dataset of Palmer Drought Severity Index for 1870–2002: Relationship with soil moisture and effects of surface warming, *J. Hydrometeorol.*, *5*, 1117–1130.
Gruber, S. (2004), Permafrost thaw and destabilization of Alpine rock walls in the hot summer of 2003, *Geophys. Res. Lett.*, *31*, L13504, doi:10.1029/2004GL020051
Guzzetti, F., S. Peruccacci, M. Rossi, and C. P. Stark (2007), The rainfall intensity-duration control of shallow landslides and debris flows: An update, *Landslides*, *5*(1), 3–17, doi:10.1007/s10346-007-0112-1.
Handwerger, A. L., J. J. Roering, and D. A. Schmidt (2013), Controls on the seasonal deformation of slow-moving landslides, *Earth Planet. Sci. Lett.*, *377–378*, 239–247, doi:10.1016/j.epsl.2013.06.047.
Handwerger, A. L., J. J. Roering, D. A. Schmidt, and A. W. Rempel (2015), Kinematics of earthflows in the Northern California Coast Ranges using satellite interferometry, *Geomorphology*, *246*, 321–333, doi:10.1016/j.geomorph.2015.06.003.
Hollingsworth, J., S. Leprince, F. Ayoub, and J.-P. Avouac (2012), Deformation during the 1975–1984 Krafla rifting crisis, NE Iceland, measured from historical optical imagery, *J. Geophys. Res.*, *117*, B11407, doi:10.1029/2012JB009140
Hungr, O., S. Leroueil, and L. Picarelli (2014), The Varnes classification of landslide types, an update, *Landslides*, *11*(2), 167–194, doi:10.1007/s10346-013-0436-y.
Iverson, R. M., and J. J. Major (1987), Rainfall, ground-water flow, and seasonal movement at Minor Creek landslide, Northwestern California: Physical interpretation of empirical relations, *Geol. Soc. Am. Bull.*, *99*, 579–594.
Kelsey, H. M. (1978), Earthflows in Franciscan melange, Van Duzen River basin, California, *Geology*, doi:10.1130/0091-7613(1978)6<361.
Klose, M. (2015), Landslide databases as tools for integrated assessment of landslide risk, *Springer Theses*.
Krzeminska, D. M., T. A. Bogaard, J. P. Malet, and L. P. H. Van Beek (2013), A model of hydrological and mechanical feedbacks of preferential fissure flow in a slow-moving landslide, *Hydrol. Earth Syst. Sci.*, *17*(3), 947–959, doi:10.5194/hess-17-947-2013.
Leprince, S., S. Barbot, F. Ayoub, and J. P. Avouac (2007), Automatic, precise, ortho-rectification and coregistration for satellite image correlation, application to ground deformation measurement, *IEEE J. Geosci. Remote Sens.*, *45*(6), 1529–1558.
Leprince, S., E. Berthier, F. Ayoub, C. Delacourt, and J. P. Avouac (2008), Monitoring Earth surface dynamics with optical imagery, *Eos Trans. AGU*, *89*(1), doi:10.1029/2008EO010001.
Mackey, B. H. (2009), The contribution of large, slow-moving landslides to landscape evolution, Univ. of Oregon.
Mackey, B. H., and J. J. Roering (2011), Sediment yield, spatial characteristics, and the long-term evolution of active earthflows determined from airborne LiDAR and historical aerial photographs, Eel River, California, *Geol. Soc. Am. Bull.*, *123*(7–8), 1560–1576, doi:10.1130/B30306.1.
Mackey, B. H., J. J. Roering, and J. A. McKean (2009), Long-term kinematics and sediment flux of an active earthflow, Eel River, California, *Geology*, *37*(9), 803–806, doi:10.1130/G30136A.1.
McSaveney, M. J., and G. A. Griffiths (1987), Drought, rain, and movement of a recurrent earthflow complex in New Zealand, *Geology*, *15*, 643–646.
Palmer, W. C. (1965), *Meteorological Drought, Weather Bureau Res. Pap., 45*, 58 pp., U.S. Dep. of Commerce, Washington, D. C.
Pelletier, J. D., et al. (2015), Forecasting the response of Earth's surface to future climatic and land use changes: A review of methods and research needs, *Earth's Future*, *3*, 220–251, doi:10.1002/2014EF000290.
Petley, D. (2012), Global patterns of loss of life from landslides, *Geology*, *40*(10), 927–930, doi:10.1130/G33217.1.
Robeson, S. M. (2015), Revisiting the recent California drought as an extreme value, *Geophys. Res. Lett.*, *42*, 6771–6779, doi:10.1002/2015GL064593.
Roering, J. J., B. H. Mackey, A. L. Handwerger, A. M. Booth, D. a. Schmidt, G. L. Bennett, and C. Cerovski-Darriau (2015), Beyond the angle of repose: A review and synthesis of landslide processes in response to rapid uplift, Eel River, Northern California, *Geomorphology*, *236*, 109–131, doi:10.1016/j.geomorph.2015.02.013.
Scherler, D., B. Bookhagen, and M. R. Strecker (2011), Spatially variable response of Himalayan glaciers to climate change affected by debris cover, *Nat. Geosci.*, *4*(3), 156–159, doi:10.1038/ngeo1068.
Schulz, W. H., J. P. McKenna, J. D. Kibler, and G. Biavati (2009), Relations between hydrology and velocity of a continuously moving landslide-evidence of pore-pressure feedback regulating landslide motion?, *Landslides*, *6*(3), 181–190, doi:10.1007/s10346-009-0157-4.
Stumpf, A., J. P. Malet, P. Allemand, and P. Ulrich (2014), Surface reconstruction and landslide displacement measurements with Pléiades satellite images, *ISPRS J. Photogramm. Remote Sens.*, *95*, 1–12, doi:10.1016/j.isprsjprs.2014.05.008.
Swain, D. L. (2015), A tale of two California droughts: Lessons amidst record warmth and dryness in a region of complex physical and human geography, *Geophys. Res. Lett.*, *42*, 9999–10,003, doi:10.1002/2015GL066628.
Terzaghi, K. (1950), *Mechanics of landslides (Berkeley volume)*, Geol. Soc. of Am., New York.
Van Asch, T. W. J., J. Buma, and L. P. H. Van Beek (1999), A view on some hydrological triggering systems in landslides, *Geomorphology*, *30*(1–2), 25–32, doi:10.1016/S0169-555X(99)00042-2.
Xia, Y., et al. (2012), Continental-scale water and energy flux analysis and validation for the North American Land Data Assimilation System project phase 2 (NLDAS-2): 1. Intercomparison and application of model products, *J. Geophys. Res.*, *117*, D03109, doi:10.1029/2011JD016048